Effect of substitution impurities and defect on structural stability and electronic properties of MoS$_2$ nanostructures: A density functional theory study

Nagarajan V., Saravanakannan V. and Chandiramouli R.[*]

School of Electrical & Electronics Engineering, SASTRA University, Tirumalaisamudram, Thanjavur, India
_____

ABSTRACT

The realistic structures of pure, Cr and Se substituted MoS$_2$ nanostructures are optimized and simulated successfully with B3LYP/ LanL2DZ basis set. The stability of MoS$_2$ nanostructures are discussed in terms of calculated energy. The point symmetry and dipole moment of both pure and impurity substituted MoS$_2$ nanostructures are also reported. The electronic properties of MoS$_2$ nanostructures are discussed by HOMO – LUMO gap, electron affinity and ionization potential. The results of the present work will give insights to tailor MoS$_2$ nanostructures by substitution impurities and defect structure which enhances the electronic properties and structural stability of MoS$_2$ nanostructures that find its key application in photo catalysis, photovoltaic cells and dry lubrication.

Keywords: molybdenum disulfide; nanostructure; dipole moment; ionization potential; electron affinity
_____

INTRODUCTION

Molybdenum disulfide (MoS$_2$) is an inorganic compound which is classified under metal dichalcogenide . Due to its robustness and low frictional properties MoS$_2$ can be used as solid lubricant. The molybdenum atoms are perfectly sandwiched between sulfur atoms to form layered structure of molybdenum disulfide and its properties resembles graphite. Graphene is one of the of two dimensional material which find its potential importance in engineering applications, but nanosheet form of transition metal disulfides (TFDs) consists of only few layer, such as tungsten disulfide (WS$_2$) and MoS$_2$. Compared to graphite, MoS$_2$ is a promising material to enhance high energy capacity. TFDs are widely used in hydro desulfurization catalysts, photo catalysis, photovoltaic cells, dry lubrication and in lithium batteries due to their optical, electronic and catalytic properties. The transition-metal dichalcogenide MoS$_2$ semiconductor has attracted many researchers due to its optical, electronic and catalytic properties [1-3]. The indirect band gap of MoS$_2$ semiconductor is 1.29 eV, the band gap of MoS$_2$ is suitable for optoelectronic, electronic and photovoltaic applications. The mono layer MoS$_2$ nanostructure has been reported recently [4] and its properties are investigated both experimentally [5-7] and theoretically [8, 9]. Moreover, recently mono layer molybdenum disulfide has been used as tunneling barrier on vertical TFET and as conductive channel in low-power field effect transistor [10]. The main goal behind this work is to optimize and enhance the optoelectronic properties and structural stability of MoS$_2$ by substituting proper impurities such as chromium and selenium. Density functional theory (DFT) is well-organized method to fine-tune electronic properties and structural stability of MoS$_2$ [11-13]. In the present work the structural stability and electronic properties of MoS$_2$ nanostructures are studied and reported.

MATERIALS AND METHODS

The hexagonal nanostructures of MoS$_2$ are completely simulated and optimized successfully using Gaussian 09W package [14]. In this work DFT method is utilized with Becke's three-parameter hybrid functional in combination with Lee-Yang-Parr correlation functional (B3LYP). The choice of basis set plays an important role in optimization

242

_____

of MoS_2 nanostructures. Since LanL2DZ is applicable to Li-La, H and Hf-Bi elements, in the present work LanL2DZ basis set is used to optimize MoS_2 nanostructures [15-18]. Gauss Sum 3.0 package [19] is used to calculate density of states (DOS) spectrum and HOMO – LUMO gap of MoS_2 nanostructures.

RESULTS AND DISCUSSION

The present work mainly focus on ionization potential (IP), dipole moment (DM), electron affinity (EA), HOMO – LUMO gap, and calculated energy of MoS_2 nanostructures with substituted impurity such as chromium, selenium and defect structured MoS_2 nanostructure. Fig. 1. (a) – Fig. 1. (c) represents pure MoS_2 – 12, pure MoS_2 – 21 and pure MoS_2 – 27 nanostructures respectively. The pure MoS_2 – 12 nanostructure has four Mo atoms and eight S atoms, pure MoS_2 – 21 contains seven Mo atoms and fourteen S atoms and pure MoS_2 – 27 consists of nine Mo atoms and eighteen S atoms to form hexagonal crystal structure with trigonal prismatic coordination geometry. Fig. 1. (d) and Fig. 1. (e) represents Cr and Se substituted MoS_2 – 12 nanostructures respectively. The defect structured MoS_2 – 12 nanostructure is shown in Fig. 1. (f). Cr substituted MoS_2 – 12 nanostructure consists of three Mo atoms, eight S atoms and one Mo atom is replaced with one Cr atom. Se substituted MoS_2 – 12 nanostructure has four Mo atoms, six S atoms and two S atoms are replaced with two Se atoms. Defect structured MoS_2 – 12 nanostructure contains three Mo atoms, six S atoms and three vacancies are created on regular arrangement of atom. Calculated energy is one of the most important key factors to find structural stability of MoS_2 nanostructures. Table 1 contains point group, dipole moment and calculated energy of MoS_2 nanostructures. The calculated energy of pure MoS_2 – 12, 21 and 27 has the value of -346.07, -605.95 and -779.24 Hartrees respectively. It shows that the stability of MoS_2 nanostructures increases with increase in number of atoms. Similarly, the stability of Cr substituted MoS_2 – 12 nanostructure slightly increases with Cr substitution. In contrast stability of defect structured MoS_2 – 12 nanostructure decreases with the presence of defect in MoS_2 – 12 nanostructure. There is no much variation in energy for Se substituted MoS_2 – 12 nanostructure, it has almost same value of pure MoS_2. The distribution of charges in MoS_2 nanostructures is inferred from dipole moment (DP). The DP of MoS_2 nanostructures slightly diverge with increasing number of atoms and also for Cr substituted MoS_2 nanostructure. The DP seems to decrease when Se is substituted in MoS_2 nanostructure. This decrease in DP arises due to electronic configuration of Se atom. The DP value of pure MoS_2 – 12, 21and 27 are found to be 19, 27.23 and 35.68 Debye respectively. It is inferred that the charge distribution is not uniform in these MoS_2 nanostructures. Cr and Se substituted MoS_2 – 12 nanostructures has the corresponding DP value of 23.94 and 15.38 Debye respectively. The DP value of defect structured MoS_2 – 12 nanostructure is 13.53 Debye. For MoS_2 nanostructures, only C_1 or C_S point symmetry is found for all pure and impurities substituted MoS_2 nanostructures. C_1 point symmetry has one symmetry operation which is identity operation (E) whereas Cs point symmetry has the identity operation (E) and a mirror plane operation (σ).
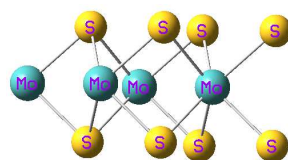
Figure 1(a). Structure of pure MoS_2 – 12 nanostructure
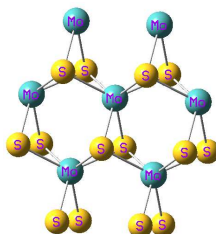

Figure 1(b). Structure of pure MoS_2 – 21 nanostructure

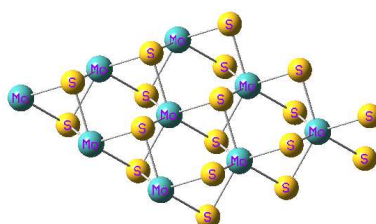**Figure 1(c). Structure of pure MoS_2 – 27 nanostructure**
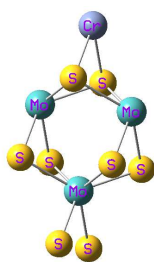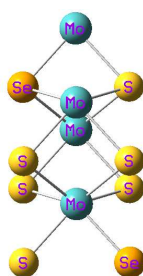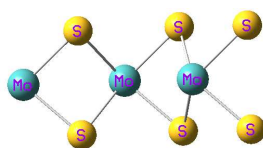
_____

Figure 1(d). Structure of Cr substituted MoS$_2$ – 12 nanostructure

Figure 1(e). Structure of Se substituted MoS$_2$ – 12 nanostructure

Figure 1(f). Defect structured MoS$_2$ - 12 nanostructure

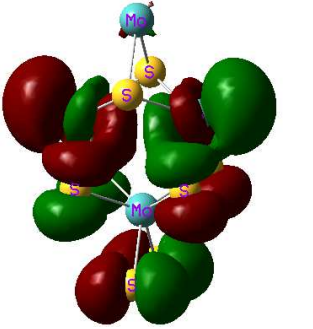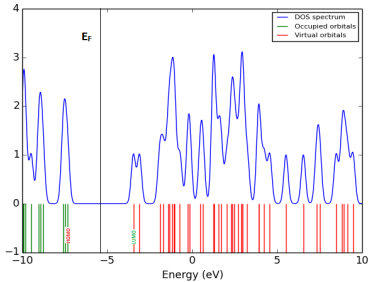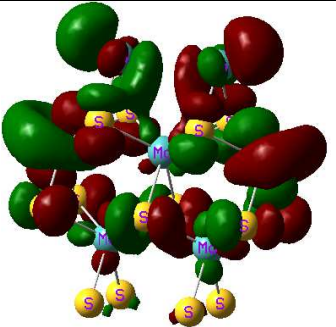**Table 1. Energy, point symmetry and dipole moment of hexagonal MoS$_2$ nanostructures**
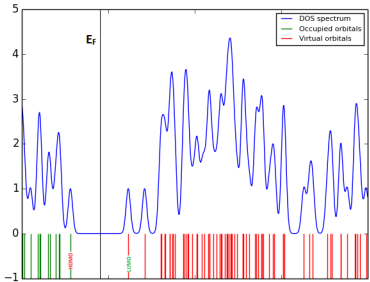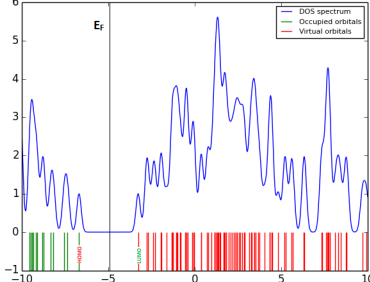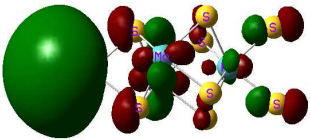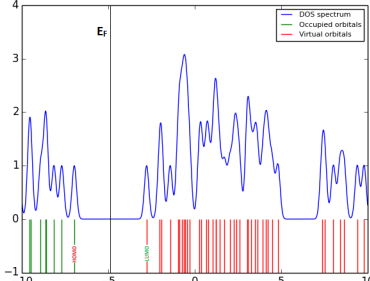
Nanostructures	Energy (Hartrees)	Dipole moment (Debye)	Point Group
Pure MoS$_2$ – 12	-346.07	19	C$_S$
Pure MoS$_2$ – 21	-605.95	27.23	C$_S$
Pure MoS$_2$ – 27	-779.24	35.68	C$_S$
Cr substituted MoS$_2$ – 12	-364.93	23.94	C$_S$
Se substituted MoS$_2$ – 12	-344.41	15.38	C$_1$
Defect structured MoS$_2$ - 12	-259.68	13.53	C$_1$

3.1. Density of states spectrum and HOMO-LUMO gap of MoS$_2$ nanostructures
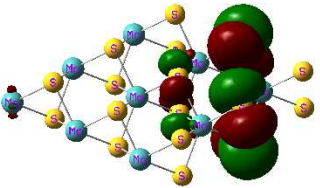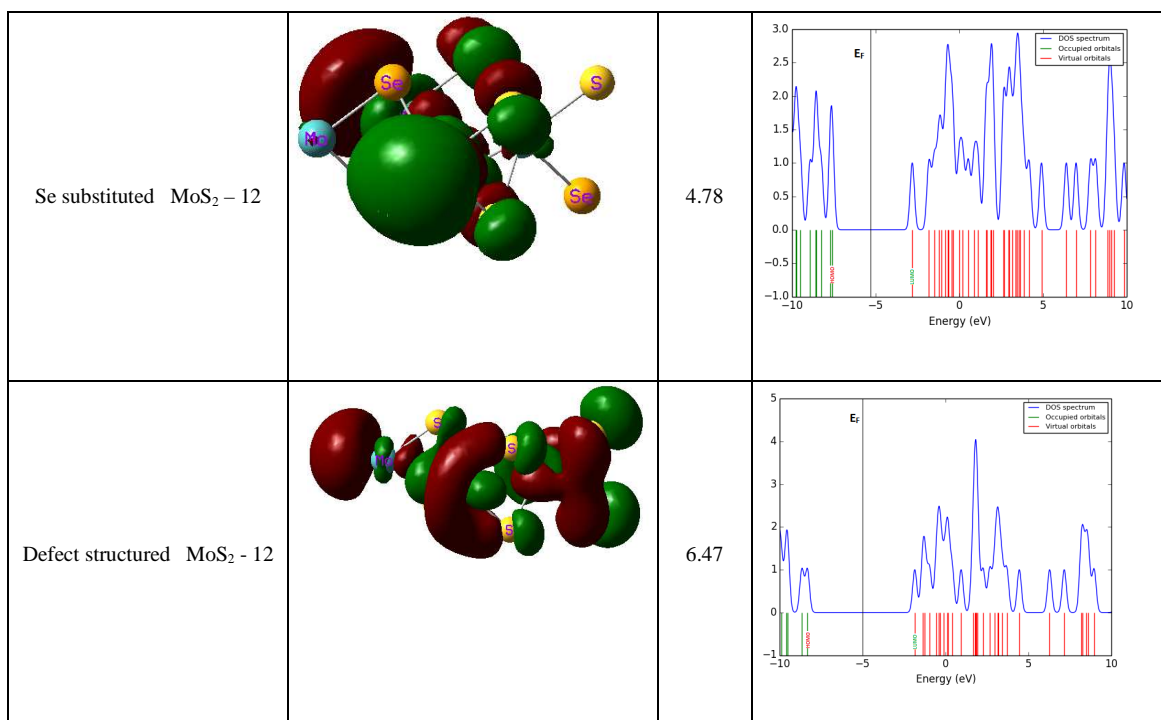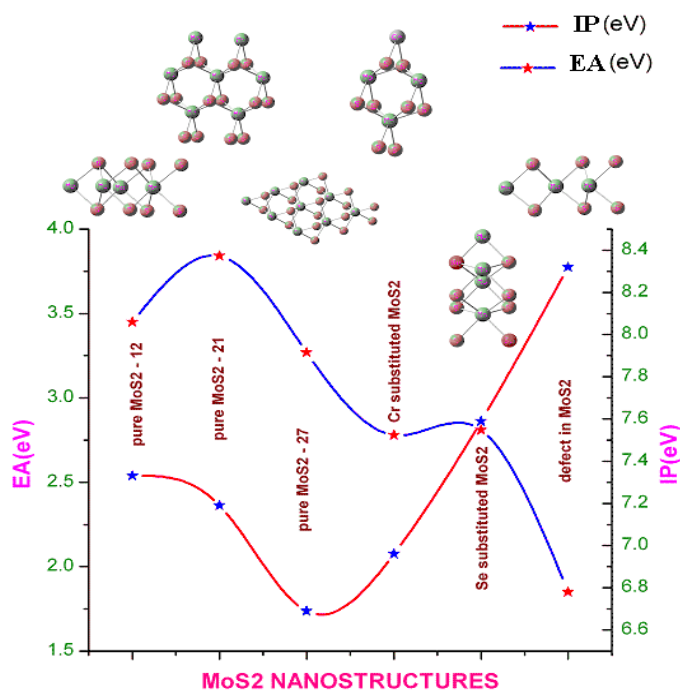
The electronic properties of MoS$_2$ nanostructures can be described in terms of highest occupied molecular orbital (HOMO) and lowest unoccupied molecular orbital (LUMO) [20-25]. The energy gap value for pure MoS$_2$ – 12, 21 and 27 is 3.88, 3.35 and 3.42 eV respectively. Depending upon the geometry of the structure, the band gap increases or decreases for MoS$_2$ nanostructures. When the energy gap increases it leads to decrease in conductivity of MoS$_2$ nanostructures. Interestingly, for Cr and Se substituted MoS$_2$ – 12 nanostructures, the energy gap further increases to 4.18 and 4.78 eV respectively. The resistivity of MoS$_2$ nanostructures gets increased due to substitution impurities. In this work theoretical band gap value of MoS$_2$ nanostructures is observed in the range of 3.35 – 3.88 eV, but the experimental direct band gap value is reported as 1.79 eV and indirect band gap value as 2.03 eV. The increase in the band gap in MoS$_2$ nanostructure arises due to the surface passivation effect of Mo and S atoms during bonding. The defect structured MoS$_2$ nanostructure has the energy gap value of 6.47 eV, the creation of vacancy at particular site in MoS$_2$ nanostructure further increases the band gap. In conclusion the electronic properties of MoS$_2$ nanostructures can be fine-tuned with increasing the number of atoms, substitution of proper impurities and by creation of defect. The tuning of band gap in MoS$_2$ leads to many application such as photo catalysis, photovoltaic cells, and in lithium batteries. Table 2 shows visualization of energy gap and density of states (DOS) spectrum. HOMO – LUMO visualization clearly reveals that the electron cloud is on occupied orbital (green color) for all possible pure and impurity substituted MoS$_2$ nanostructures. This refers the occupancy of electron in occupied orbitals. In contrast the electron cloud is more in virtual orbital (red color) for defect structured MoS$_2$ nanostructure

244

_____

due to wide band gap. The DOS spectrum shows more peaks in virtual orbitals than occupied orbitals. These peak maximum arises due to the overlapping of Mo electronic orbitals with S orbitals. This infers the localization of charges in the virtual orbital [26-29].

Table 2. HOMO-LUMO gap and density of states of MoS$_2$ nanostructures

Nano structures	HOMO – LUMO Visualization (HOMO / LUMO)	E$_g$ (eV)	HOMO, LUMO and DOS Spectrum
Pure MoS$_2$ - 12		3.88	
Pure MoS$_2$ – 21		3.35	
Pure MoS$_2$ – 27		3.42	
Cr substituted MoS$_2$ – 12		4.18	

_____

Se substituted MoS$_2$ – 12		4.78	
Defect structured MoS$_2$ - 12		6.47	

Fig. 2. IP and EA of MoS$_2$ nanostructures

3.2. Ionization potential, electron affinity of MoS$_2$ nanostructures

The electronic properties of all the possible pure and impurity substituted MoS$_2$ nanostructures can be described through electron affinity (EA) and ionization potential (IP) [30, 31]. Figure 2 implies the graphical representation of EA and IP of MoS$_2$ nanostructures. The energy required to eject electron from MoS$_2$ nanostructures are known as IP. EA is energy released due to adding of electron in MoS$_2$ nanostructures. Almost same trends are observed in IP which ranges in the order of 6.69 to 7.59 eV except for defect structured MoS$_2$ nanostructure which has the value of 8.32 eV. IP value for pure MoS$_2$ – 12, 21 and 27 nanostructures are 7.33, 7.19 and 6.69 eV respectively. For Cr and Se substituted MoS$_2$ nanostructures, the corresponding IP value is 6.96 and 7.59 eV respectively. It is inferred that the IP value of MoS$_2$ nanostructures get decreases due to increase in number of atoms and also with Cr substitution.

246

_____

In these MoS_2 nanostructures, small amount of energy is enough to remove electron. In the case of Se substituted and defect structured MoS_2 nanostructures the value of IP is high. Electron affinity plays a vital role in chemical sensors and in plasma physics. Almost the same trend is observed in EA for MoS_2 nanostructures. The EA value for pure and impurity substituted MoS_2 nanostructure has the value in the range of 2.81 – 3.84 eV except for defect structured MoS_2 nanostructures which has the value of 1.85 eV. Only small amount of energy is released from MoS_2 nanostructures due to addition of electron in appropriate site.

CONCLUSION

Using DFT, pure, Cr and Se substituted and defect MoS_2 nanostructures are optimized and simulated successfully with B3LYP /LanL2DZ basis set. The structural stability of MoS_2 nanostructures are discussed using calculated energy. Point symmetry group and dipole moment of all MoS_2 nanostructures are reported. With the help of HOMO – LUMO gap, electron affinity and ionization potential, electronic properties of all realistic MoS_2 nanostructures are studied. The present work reveals that the structural stability and electronic properties can be enhanced in MoS_2 nanostructures by properly tailoring with substitution of Cr and Se impurities. The influence of defect in MoS_2 is also discussed. Moreover, the electronic properties and structural stability of MoS_2 nanostructures can be enhanced with proper substitution or creating the defect in the structure that find its potential importance in photo catalysis, photovoltaic cells and dry lubrication.

REFERENCES

[1]T.S. Li, G.L.Galli, *The journal of physical chemistry C .*, **2007**, 111 (44) 16192.
[2] S. Lebegue, O.Eriksson, *Physical Review B.,* **2009**, 79, 115409.
[3] X. Zong, *Journal of American Chemical Society.,* **2008**, 130, 7176.
[4] K.S.Novoselov, D. Jiang, F. Schedin, T.J. Booth, V.V. Khotkevich, S.V. Morozov, A.K. Geim, *Proceedings of the National Academy of Sciences USA.,* **2005**, 102, 10451.
[5] K.F. Mak, C. Lee, J. Hone, J. Shan, T.F. Heinx, *Physical Review Letters.*, **2010**, 105, 136805.
[6] A. Splendiani, L. Sun, Y.Zhang, T. Li, J. Kim, C.Y. Chim, G. Galli, F. Wang, *Nano letters.,* **2010**, 10, 1271.
[7] S.W. Han, H. Kwon, S.K. Kim, S. Ryu, W.S. Yun, D.H. Kim, J.H. Hwang, J.S. Kang, J. Baik, H.J. Shin, S.C. Hong, *Physical Review B.,* **2011**, 84, 045409.
[8] T.Li, G.Galli, *Journal of Physical Chemistry C.,* **2007**, 111, 16192.
[9] C. Ataca, H. Sahin, E. Akturk, S. Ciraci, *Journal of Physical Chemistry C.,* **2011**, 115, 3934.
[10] B. Radisavljevic, A. Radenovic, J. Brivio, V. Giacometti, A. Kis, *Nature Nanotechnology.,* **2011**, 6, 147.
[11] V.Ganesan, V.Nagarajan, V.Saravanakannan, R.Chandiramouli, *Int.J. ChemTech Res.*, **2014**, 6 (7), 3822.
[12] V.Nagarajan, R. Chandiramouli, *Ceram. Int.*, **2014**, 40, 16147.
[13] V.Nagarajan, R. Chandiramouli, *Computational and Theoretical Chemistry.*, **2014**, 1049, 20.
[14] M. J. Frisch, G. W. Trucks, H. B. Schlegel, G. E. Scuseria, M. A. Robb, J. R. Cheeseman, G. Scalmani, V. Barone, B. Mennucci, G. A. Petersson, H. Nakatsuji, M. Caricato, X. Li, H. P. Hratchian, A. F. Izmaylov, J. Bloino, G. Zheng, J. L. Sonnenberg, M. Hada, M. Ehara, K. Toyota, R. Fukuda, J. Hasegawa, M. Ishida, T. Nakajima, Y. Honda, O. Kitao, H. Nakai, T. Vreven, J. A. Montgomery, Jr., J. E. Peralta, F. Ogliaro, M. Bearpark, J. J. Heyd, E. Brothers, K. N. Kudin, V. N. Staroverov, R. Kobayashi, J. Normand, K. Raghavachari, A. Rendell, J. C. Burant, S. S. Iyengar, J. Tomasi, M. Cossi, N. Rega, J. M. Millam, M. Klene, J. E. Knox, J. B. Cross, V. Bakken, C. Adamo, J. Jaramillo, R. Gomperts, R. E. Stratmann, O. Yazyev, A. J. Austin, R. Cammi, C. Pomelli, J. W. Ochterski, R. L. Martin, K. Morokuma, V. G. Zakrzewski, G. A. Voth, P. Salvador, J. J. Dannenberg, S. Dapprich, A. D. Daniels, Ö. Farkas, J. B. Foresman, J. V. Ortiz, J. Cioslowski, and D. J. Fox, Gaussian, Inc., Wallingford CT, **2009**.
[15] R.Chandiramouli , *Res. J. Chem. Environ.*, **2013**, 17, 64.
[16] V.Nagarajan, R. Chandiramouli , *Int.J. ChemTech Res.*, **2014**, 6(4), 2240.
[17] V.Nagarajan, R. Chandiramouli, *Alexandria Engineering Journal.*, **2014**, 53, 437.
[18] R.Srinivasaraghavan, R. Chandiramouli , B.G.Jeyaprakash, S. Seshadri, *Spectrochim. Acta, Part A.*, **2013**, 102, 242.
[19] N.M.O'boyle, A.L.Tenderholt, K.M.Langner, *J. Comput. Chem.*, **2007**, 29, 839.
[20] V. Nagarajan, R. Chandiramouli, *Struct Chem.*, **2014**, 25, 1765.
[21] V. Nagarajan, R. Chandiramouli, *J Inorg Organomet Polym.*, **2014**, 24, 1038.
[22] V.Ganesan, V.Nagarajan, V.Saravanakannan, R.Chandiramouli, *Int.J. ChemTech Res.*, **2014**, 6(7), 3832.
[23] S.Sriram, R.Chandiramouli, D.Balamurugan, A. Thayumanvan, *Eur. Phys. J. Appl. Phys.*, **2013**, 62, 30101.
[24] V.Nagarajan, V.Saravanakannan, R.Chandiramouli, *Int.J. ChemTech Res.*, **2014**, 6(5), 2962.
[25] V.Nagarajan, R.Chandiramouli, *Res J Pharm BiolChemSci*, **2014**, 5(1), 365.
[26] R.Chandiramouli, S.Sriram, D.Balamurugan, *Mol. Phys.*, **2014**, 112, 151.
[27] V.Nagarajan, R. Chandiramouli, *J Inorg Organomet Polym.,* **DOI**: 10.1007/s10904-015-0167-8.
[28]V. Nagarajan, R. Chandiramouli, *Superlattices Microstruct.*, **2015**, 78, 22.

_____

[29] S.Sriram, R.Chandiramouli, B.G.Jeyaprakash, *Struct Chem.*, **2014**, 25, 389.
[30] V.Nagarajan, R.Chandiramouli, *Der PharmaChemica.*, **2014**, 6 (1), 37.
[31] V.Nagarajan, R.Chandiramouli, *Int.J. ChemTech Res.,* **2014**, 6(1), 21.